

Numerical implementation of a sparse grid for a hyperbolic geophysical mass flow model

E. R. Stefanescu¹, A.K. Patra¹, K.R. Dalbey², and M. Bursik³

¹Department of Mechanical and Aerospace Engineering, University at Buffalo

²Sandia National Labs, Albuquerque

³Department of Geology, University at Buffalo

November 4, 2011

1 Introduction

This paper describes the development of sparse grid based methodology for the propagation of input parameter uncertainties through a shallow-water like hyperbolic system model of geophysical mass flows. We apply the sparse grid based methodology first to the straightforward analysis of UQ in the output of the model and then to the more complex construction of hazard maps based on the outcomes of ensembles of model runs. The results are interesting in that they show that the sparse grid method is quite successful in the first type of analysis where the uncertainty in a number of flow outcomes are successfully captured but the results from the hazard map construction that requires a more extensive exploration of the full parameter space to construct a response surface is not as successful.

1.1 Background

1.1.1 Geophysical aspect

In geophysical mass flow problems (e.g. landslides, volcanic debris flows called lahars), many flow characteristics like material properties, the size and location of failing mass, the terrain over which the flow occurs at every point in the domain are difficult if not impossible to characterize. There is also much that is unknown about the exact physics. Thus, useful outputs from the model equations governing mass flow must account for the variable or poorly characterized aspects of the model as well as the uncertainty of the parameters used in the equations (3). Most of the numerical models of real-world systems are characterized by large number of input variables. In this case, to obtain a reliable numerical solution, one has to include uncertainty quantification due to the uncertainty in the input data. Furthermore, in many use situations of geophysical mass

flows, one is concerned with flow over an entire jurisdiction (hazard analysis). This introduces additional complexity in the propagation of the uncertainty.

1.1.2 Uncertainty Quantification Methods

Quantification of uncertainty means to be in some way able to attach a measure to something which may be poorly defined or vague (8; 10) – in this case the outcomes of models with uncertain inputs. To quantify the uncertainties in the result of a simulation, one must understand both the sources of these uncertainties, and how uncertainties propagate through the simulation. Uncertainty quantification thus involves two steps: determination of the uncertainty sources, and analysis of their propagation through the simulation. In the past few years there have been extensive studies in the propagation of uncertainty. The common stochastic methods can be categorized in sampling and non-sampling methods. Widely used sampling methods are: Monte-Carlo(MC), quasi-Monte Carlo (QMC), Latin Hypercube sampling (LHS), while as non-sampling methods intensively used are: Polynomial Chaos Expansion (PCE), Stochastic Galerkin (SG), Non-Intrusive Spectral Projection (NISP), Polynomial Chaos Quadrature (PCQ) etc.

MC methods have been applied to many applications and their implementation is straightforward. Although the convergence rate is relatively slow, it is independent of the dimensionality of the random space and independent of the number of random variables used to characterize the random inputs. To accelerate convergence in MC, several techniques have been developed as LHS and QMC. The PCE method uses the Wiener-Askey scheme, in which Hermite, Legendre, Laguerre, Jacobi, and generalized Laguerre orthogonal polynomials are used for modeling the effect of uncertain variable described by normal, uniform, exponential, beta, and gamma distributions, respectively (4; 7). These orthogonal polynomial selections are optimal for these distribution type since the inner product weighting function and its corresponding support range correspond to the probability density functions for these continuous distributions. PCQ is based on the PCE in general and on SG in particular. The main idea is that in addition to calculating the coefficients in the expansion of chaos polynomials, PCQ achieves a more accurate computation of statistical moments when the governing system of equations is non-polynomial, by calculating the moments directly rather than through the intermediate coefficients (6; 5). These concepts has been used successfully in many engineering approaches over the past two decades. All methods have positive and negative features, and no single technique is optimum for all situations.

Recently, a stochastic collocation scheme has been introduced in which simulations are performed at specific collocation points in the stochastic space. Stochastic collocation methods for sPDEs have been first proposed by using numerical quadrature for the approximate evaluation of the stochastic integrals. These technique combine the exponential convergence rate of the PCE scheme with the decoupled nature of MC techniques. The selection of computational nodes is the key ingredient in all stochastic colocation methods. Choices of collocation points include tensor product of zeros of orthogonal polynomials, sparse grid (SP) methods, and probabilistic collocation.

This paper presents an approach to characterize the effect of the input uncertainty on the output of a geophysical mass flow model. We use the concept of stochastic collocation to account

for uncertainties in a non-linear hyperbolic system of PDEs used in modeling geophysical mass flow. Neglecting the model uncertainty we focus on the input parameter uncertainty, modeled as random variables. Geological flow models are dealing with high dimensional input. There are large uncertainties associated with the construction of the DEMs and many other parameters that characterize the flow.

We first discuss sparse grid algorithms as an improvement of the MC, LHS and PCQ methods. The sparse grid scheme are chosen based on their efficiency which in most of the cases results in a number reduction of collocation points needed to obtain a given level of approximation. Further, a stochastic space is defined for each problem depending on the uncertainty in parameters. Computational points are identified in this stochastic space and simulations of the geophysical flow model are performed. Our goal is to compute the statistics of the output in form of mass velocity, maximum height of the pile over time, momentum etc and compare the convergence for the above mentioned methods.

Sparse grid schemes have been successfully implemented for parabolic and elliptic sPDEs. It was proposed a framework combining space-time multigrid methods with sparse grid collocation techniques to solve a nonlinear parabolic system with random coefficients, while Babuska proposed a stochastic collocation method to solve elliptic partial differential equations with random coefficients and forcing terms. In the paper of a numerical simulations is done for an incompressible and slightly compressible single and the two-phase flow in porous media. The stochastic domain is represented using collocation at the zeros of tensor product Hermite polynomials. It was observed that the stochastic collocation converges much faster (to the mean and variance) than the standard MC approach with a significantly reduced number of simulations. In the literature it was made a comparison of the accuracy and efficiency of the sparse grid collocation approach to MC and GPCE is performed, when used to solve a natural convection problem.

In the paper, we also propose to investigate the use of sparse grid design (SPD) for hazard map construction. Sparse grids provide sampling points which avoid the curse of dimensionality. A Bayes Linear Model (BLM) is used to fit the data and construct a hazard map.

The paper is organized as follows: we first give a brief description of the non-linear hyperbolic systems used in modeling geophysical mass flows. Then we proceed to discuss sparse grid schemes in section 3 and details of numerical implementation in section 4. Finally discussions and conclusions are presented in section 5.

2 Basic model

2.1 Governing equations

The geophysical mass flow code - TITAN2D combines numerical simulations of the flow with digital data of the natural terrain. It is based on a depth-averaged model for an incompressible granular material, governed by Coulomb-type friction interactions (12). The governing equations are obtained by applying conservation laws to the incompressible continuum, providing appropriate constitutive modeling assumptions, and then taking advantage of the shallowness of the

flows (flows are much longer and wider than they are deep) to obtain simpler depth-averaged representations (11). The motion of the material is considered to be gravitationally driven and resisted by both internal and bed friction forces. The stress boundary conditions are: no stress at the upper free-surface and a Coulomb-like friction law imposed at the interface between the material and the basal surface. The resulting hyperbolic system of equations is solved using a finite-volume scheme – with a second-order – Godunov solver. Even if many real geophysical flows such as debris flow are fluidized, in this study we deal only with granular material that has not been fluidized.

$$\begin{aligned} \frac{\partial h}{\partial t} + \frac{\partial(V_x \cdot h)}{\partial x} + \frac{\partial(V_y \cdot h)}{\partial y} &= 0 \\ \frac{\partial hV_x}{\partial t} + \frac{\partial(V_x \cdot hV_x + 0.5k_{ap}g_zh^2)}{\partial x} + \frac{\partial(V_y \cdot hV_x)}{\partial y} &= S_x \\ \frac{\partial hV_y}{\partial t} + \frac{\partial(V_x \cdot hV_y)}{\partial x} + \frac{\partial(V_y \cdot hV_y + 0.5k_{ap}g_zh^2)}{\partial y} &= S_y \end{aligned} \quad (1)$$

where

$$k_{ap} = 2 \frac{1 \mp \sqrt{1 - \cos^2(\phi_{int})(1 + \tan^2(\phi_{bed}))}}{\cos^2} - 1$$

The source terms are defined as:

$$\begin{aligned} S_x &= g_x h - \frac{V_x}{\sqrt{V_x^2 + V_y^2}} \max\left(g_z + \frac{V_x^2}{r_x}, 0\right) h \tan((\phi_{bed}) - \operatorname{sgn}\left(\frac{\partial V_x}{\partial y}\right) h k_{ap} \frac{\partial(g_x h)}{\partial y} \sin((\phi_{int}) \\ S_y &= g_y h - \frac{V_y}{\sqrt{V_x^2 + V_y^2}} \max\left(g_z + \frac{V_y^2}{r_y}, 0\right) h \tan((\phi_{bed}) - \operatorname{sgn}\left(\frac{\partial V_y}{\partial x}\right) h k_{ap} \frac{\partial(g_y h)}{\partial x} \sin((\phi_{int})) \end{aligned} \quad (2)$$

where, h is the height of the flow, hV_x, hV_y are moments in x and y directions, $g = \{g_x, g_y, g_z\}$ are components of the gravity along the three axes. ϕ_{int} and ϕ_{bed} are the internal and basal friction angles, respectively, and r_x and r_y are the radii of curvature of terrain in the x and y directions.

2.2 Parameters uncertainty

TITAN2D was developed for modeling dry geophysical granular flows, such as debris avalanches and block and ash flows. Given a digital elevation map specifying the topography of a volcano and the values of input parameters, including the initial volume of erupted material and the friction angles, TITAN2D calculates the flow depth and velocity at any location throughout the

duration of an event. There is uncertainty in all of the input parameters. It was found by (Keith) that the flow is fairly insensitive to internal friction angle, but bed friction angle and the size of the initial flowing mass are important. The degree of sensitivity to initial location highly depends on the local terrain features in the neighborhood of the starting location. The combination of uncertainty and sensitivity to these inputs dictates which ones need to be represented as random variables.

3 Stochastic numeric methods

To account for the impact of the uncertainty in the parameters, it is natural to consider moments of the solutions over the probabilistic space. In other words, we need to evaluate multi-dimensional integrals. The main idea of the stochastic collocation approach is to abandon the random sampling approach and consider the use of the more advanced integration approaches as hierarchical integration techniques.

We are interested in convergence of the first and second moment of the model output when using sparse grid as a colocation method. In an attempt to minimize the number of sample points we use sparse grid schemes. The colocation points in the high-dimensional random parameters space is significantly reduced compared to a full tensor product.

The MC, LHS, PCQ and SP approaches follow identical procedures except in the choice of grid points in the sample space and the quadrature weights associated with those points. These procedures and the choices of collocation points for the SP are described below.

3.1 Monte Carlo simulations

In a typical MC simulation with N_{MC} number of samples the mean converges asymptotically as $\sqrt{N_{MC}^{-1}}$, and is independent of the number of random dimensions, N . The general procedure for MC simulation of transport equations is:

- Generate N_{MC} sample
- Solve the deterministic problem for each sample
- Stochastic moments are computed as simple arithmetic means

$$\langle U(\xi_{i=1 \dots N_{MC}})^N \rangle = \frac{1}{N_{MC}} \sum_{i=1}^{N_{MC}} U(\xi_i)^N \quad (3)$$

The mean is given as $\text{mean}(U) = \langle U \rangle$. By the central limit theorem (Chung, and more) the accuracy is $\frac{\sigma}{\sqrt{N_{MC}}}$, where σ is the standard deviation of the estimate. Thus to double the accuracy, it is necessary to quadruple the number of sample points.

3.2 Latin Hypercube Sampling

The Latin Hypercube Sampling is implemented as bellow:

- For each random dimension/variable generate N_{pts} .
- For every $i = 1, \dots, N_{pts}$ points, one value from each of the N_{dir} random direction is taken to form the coordinates of the point in the N_{dir} -dimensional sample space.
- Evaluate the model for this value of the sample space.
- Expectations and other statistics are calculated as in MC.

3.3 PCQ

PCQ is natural evolution of the SG, only that the evaluation of the projections is performed through quadrature - that is, via numerical rather than analytical integration. It leads to a method that has the simplicity of MC and cost of PC.

3.4 Sparse grid collocation method

3.4.1 One dimension

A general univariate integration problem can be written as :

$$I[g] = \int_{\Omega} g(x)w(x)dx \quad (4)$$

Where x represents a random variable, $g(x)$ is a function in x and $w(x)$ represents the p.d.f. of x with support Ω . The polynomial-based approaches fit polynomials to the integrand, and the resulting polynomial function is then integrated. In general, the nodes are the roots of the fitted polynomials. A sequence of quadrature rule is defined $V = \{V_i : i \in N\}$ and each rule V_i specifies a set of rule $X_i \subset R$ and a corresponding weight function $w_i : X_i \rightarrow R$. The optimal abscissas of the n -point Gaussian quadrature formulas are the roots of an orthogonal polynomial for the same interval and weighting function. In this case the approximation of I by V_i is given as :

$$V_i[g] = \sum_{x \in X_i} g(x)w_i(x)dx \quad (5)$$

Gauss-Legendre

Gaussian quadrature is the best known polynomial-based method, famed for its $2n - 1$ degree of polynomial exactness, meaning that with n function evaluations, all integrands which are polynomials of order $2n - 1$ or less will be integrated exactly. Gaussian quadrature utilizes orthogonal polynomials, such as Legendre, Hermite, or Laguerre polynomials. When approximating expectations of functions of random variable, the choice of orthogonal polynomial should reflect the type of random variable. Legendre polynomials should be used for uniform random variables, and Hermite polynomials for normal random variables. However, the Gauss-Legendre formulas are in general not nested.

Gauss-Kronrod-Patterson quadrature rules

Gauss-Kronrod-Patterson quadrature are an extension of Gaussian rules first developed by Kronrod and then iterated by Patterson to yield a sequence of nested quadratures: the set of nodes for each level are contained in the nodes for all successive levels. In the sparse grid formulation nesting allows function evaluations to be reused. Thus, the n -point Gauss quadrature formula was extended by $n+1$ points (zeros of the Stieltjes polynomials such that the polynomials) degree of exactness or the resulting $2n+1$ formula is maximal.

Clenshaw-Curtis

The nodes of Clenshaw-Curtis quadrature are at the roots of Chebyshev polynomials and is exact for polynomial of order n when $n+1$ points are used. For a given level $k \in N$ the sequence of n_k -point quadrature formula is:

$$n_k = \begin{cases} 2^{k-1} + 1 & \text{if } k > 1 \\ 1 & \text{if } k = 1 \end{cases} \quad (6)$$

And the abscissas are given by:

$$x_{ki} = \begin{cases} -\frac{1}{2} \cdot (\cos \frac{\pi \cdot (i-1)}{n_k-1} + 1) & \text{for } k = 1, \dots, n_k, \text{ if } n_k > 1 \\ 1 & \text{for } k = 1, \text{ if } n_k = 1 \end{cases} \quad (7)$$

When considering the efficiency of the integration measured through polynomial exactness, it is worth keeping in mind that polynomial exactness is just one measure of accuracy and making other choices may well better highlight the advantages of other methods. It was shown by that the Clenshaw-Curtis very often is comparable or even better in accuracy to Gauss quadrature despite formally having lower polynomial exactness. This behavior will be observed in section 4 in the construction of the hazard map.

3.4.2 Multiple dimensions

The extension of the univariate quadrature rules to multiple dimensions can be achieved by the product rule.

Full Grids

The use of a full tensor product space is attractive in the case of a small number of random variables. In D dimensions, the number of evaluations of the function grows exponentially and as dimension grows, the error order grows as well at an exponential rate: $\mathcal{O}(n_q^{-r/D})$. This is defined for functions in C^r (function with bounded mixed derivatives up to order r) and where n_q is the total number of points in the grid. If the number of random variables is moderate or large, one should rather consider full polynomial space or sparse tensor product spaces.

Sparse Grids

Smolyak (1963) introduced what is now known as Smolyak's formula and is the underlying formulation of all sparse grid methods (MITsp and more). Define the level i difference quadrature:

$$\Delta_i = V_i - V_{i-1}, \quad V_0 = 0 \quad \forall i \in N \quad (8)$$

With $\mathbf{i} = [i_1, \dots, i_D]$, define for any $q \in N_0$:

$$N_q^D = \{\mathbf{i} \in N^D : \sum_{d=1}^D i_d = D + q\} \quad (9)$$

and $N_q^D = \emptyset$ for $q \leq 0$.

The Smolyak rule with accuracy level $k \in N$ for D-dimensions:

$$A_{D,k}[g] = \sum_{q=0}^{k-1} \sum_{\mathbf{i} \in N_q^D} (\Delta_{i_1} \otimes \dots \otimes \Delta_{i_D})[g] \quad (10)$$

The above rule was improved by (Wasilowki) by expressing $A_{D,k}[g]$ directly in terms of the univariate quadrature rules instead of their differences.

$$A_{D,k}[g] = \sum_{q=k-D}^{k-1} (-1)^{k-1-q} \binom{D-1}{k-1-q} \sum_{\mathbf{i} \in N_q^D} (V_{i_1} \otimes \dots \otimes V_{i_D})[g] \quad (11)$$

It can be seen that nesting causes points of different grids in the sum to coincide, and the number of common points increases with both the level and dimension of the sparse grid (Fig. 1). The error for a sparse grid can be estimate as:

$$|I[g] - A_{D,q}[g]| = \mathcal{O}(n_q^{-r} \log(n_q)^{(D-1)(r+1)}) \quad (12)$$

The advantage of the stochastic collocation approach on sparse grids with respect to, e.g., Monte Carlo simulation, is to reduce the number of solver calls. The Smolyak algorithm provides a way to construct interpolation functions based on a minimal number of points in multi-dimensional space. When one is dealing with multiple stochastic dimensions, it is straightforward to extend the interpolation functions in the one dimension to multiple dimensions by using tensor products in this special way. The algorithm provides a linear combination of tensor products chosen in such a way that the interpolation error is nearly the same as the full-tensor product in higher dimensions.

4 Numerical implementation

Inputs to the TITAN2D code are the size and the location of the mass at initiation, internal and bed friction angle, and a digital elevation map (DEM) of the topography. One of the output file produced by the code contains the mass averaged velocity and maximum height of the pile.

As a first step of the analysis, a sparse grid implementation is used to propagate the input parameter uncertainties through a shallow-water like hyperbolic system model of geophysical mass flows. High order moments of the output were calculated. We are going to illustrated the MC, LHS and PCQ for the granular flow equations as applied to a slumping flow of a cylinder of granular material. In this paper, a comparison on the convergency of the mean and standard deviation is performed for the case when we are dealing with 2 and 4 random input parameters.

Since many of the modeling applications are characterized by large number of input variables, TITAN2D being also the case, we try to explore the high-dimensional input variable space and its impact on the model. An important concern is the number of experiment or modeling simulations necessary to learn the effect of the system input on the output behavior. Full space analysis without any a priori assumption has an exponential growing computational complexity, which leads to some "smart" way of sampling the parameter space. In the paper, we implemented a Sparse Grid Design (SPD) and LHS.

The following steps were performed in the analysis:

- Collocation points were generated in the stochastic domain at different level of accuracy. The sparse grid toolkit *spinterp* is employed for this purpose.
- Weights corresponding to each collocation point are determined.
- At each collocation point, TITAN2D simulations are performed and the relevant outputs are stored.
- A comparison of the outputs is done for each study case.

4.1 Slumping pile - 2 RV

We considered the case of a cylindrical pile of granular material, with a 10 cm height and radius, resting on a horizontal surface that is suddenly released. The bed and internal friction angles have random distributions:

$$\phi_{bed} = (20 + 5\xi_1) \frac{\pi}{180} \quad (13)$$

$$\phi_{int} = \phi_{bed} + (5 + 3\xi_2) \frac{\pi}{180}$$

were ξ_1 and ξ_2 are uniform distributed between -1 and 1. We are using a Gauss-Legendre and Kronrod-Gauss-Paterson type sparse grid to calculate the mean and the standard deviation of averaged velocity and maximum pile height of the pile after 3.0 seconds. Figure 2 and 3 show the way the simulations points are distributed in the input space.

4.2 Slumping pile - 4 RV

The random variables in this study case are $\phi_{bed} \sim \mathcal{U}(15-22)$, $\phi_{int} \sim \mathcal{U}(20-34)$, and the volume of the initial pile. The shape of the initial failure region is approximated as a paraboloid and gives a good approximation of the volume range. The radius values were uniformly distributed between 10 and 20 mm, while the initial height followed the same distribution with values between 10 and 20 mm. Additional to SP runs, MC, LHS and PCQ simulations were performed.

4.3 Real study case

In the next step of our analysis we applied the computational model to a more complex scenario. In this case are dealing with the digital terrain representation of Mammoth Mountain, which is

a large, geologically young volcano located on the southwestern rim of the Long Valley Caldera, California (1). Along with uncertainties in the DEM, other four parameters are used to set the bounds of the computational modeling: internal friction angle, basal friction angle, volume of the flows, and location of the initial pile. Based on the knowledge acquired from the domain expert involved in the analysis and previous work in hazard analysis using TITAN2D, we chose parameters for the flow models to bracket the range of flow volumes and to be representative of the friction angles that have been used by other researchers in their computational models. Many TITAN2D users have chosen values of internal friction that range between 15 and 37 degrees with values between 30 and 35 being the most frequent values used (11; 9). For our study we use an internal friction angle uniformly distributed between 20 and 25 degrees. We are using a basal friction angle uniformly distributed between 15 and 20 degrees. Block and ash flows on Mammoth Mountain might contain $O(10^5 - 10^7)m^3$ of material (11; 2). Thus, our choice of volumes ranges from 1.9×10^5 to $5 \times 10^6m^3$. Initiation locations were taken from previous mapping of vent sites, coupled with knowledge of known weak areas within the volcano as indicated by hydrothermal alteration. Around the centers of the separate initiation locations, different starting positions were uniformly distributed in a circle of radius 200 m.

??For a better understanding of the effect of the increase in dimension of the input space simulation for 4 RV, and 8 RV were performed.

5 Results and Conclusions

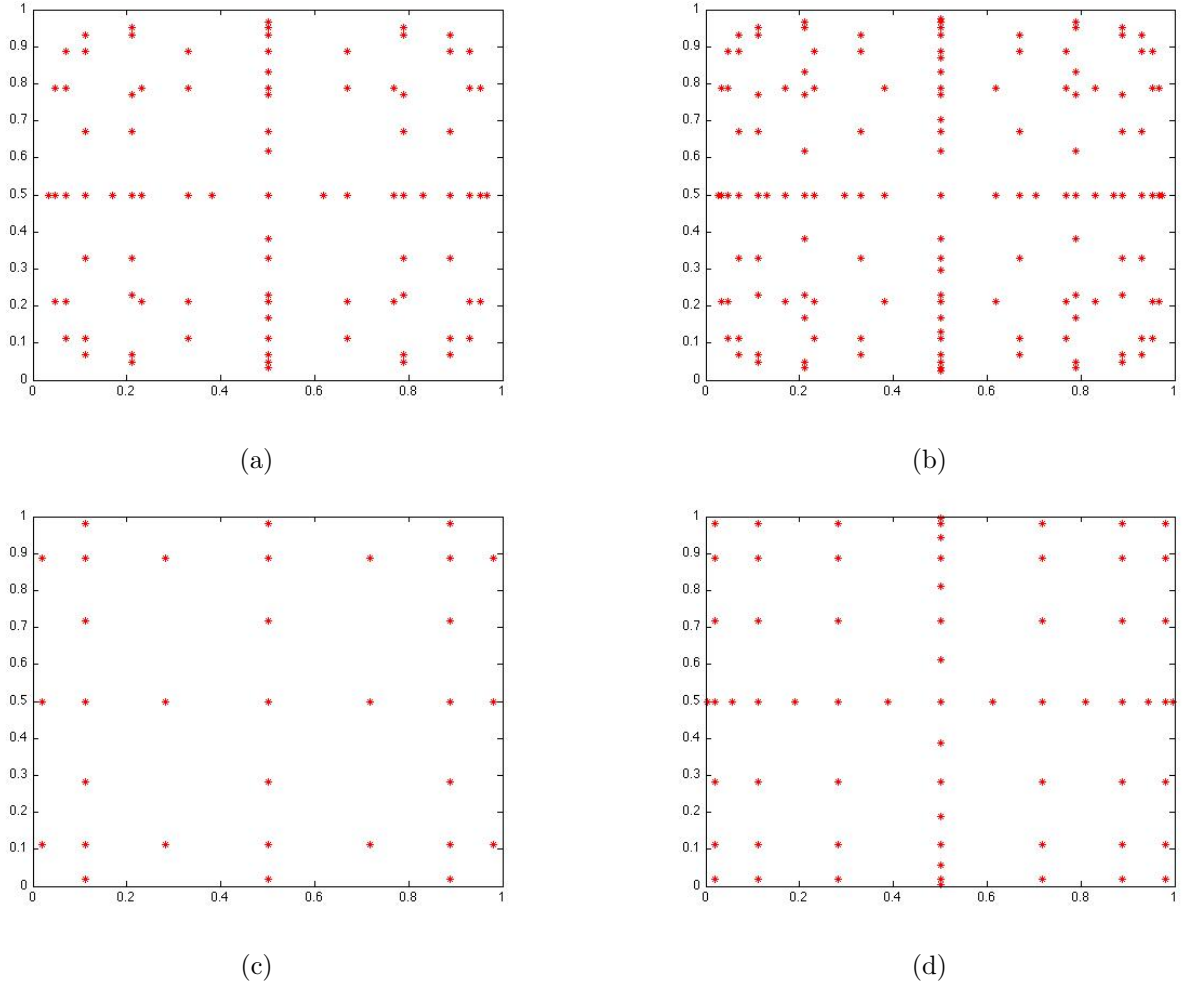
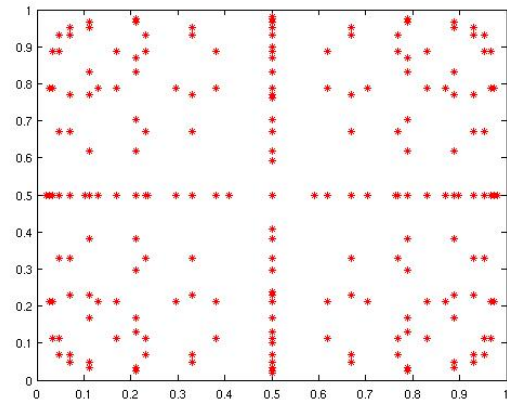
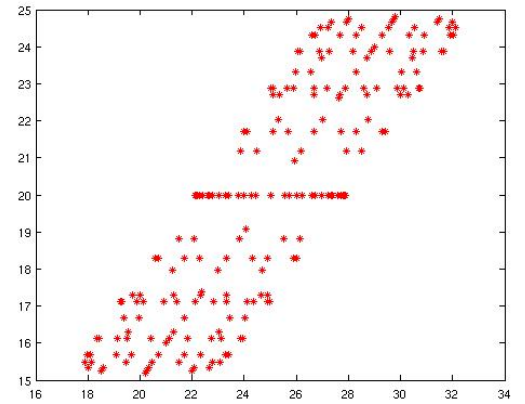


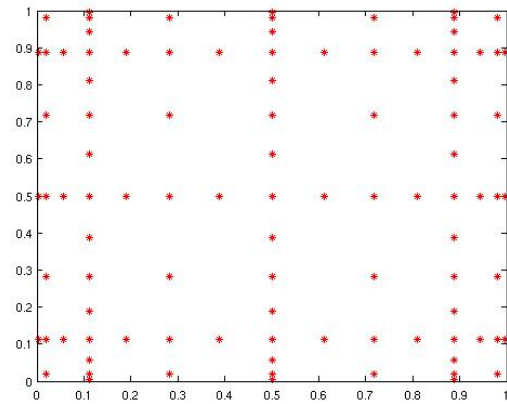
Figure 1: (a) Gauss-Legendre level 6 of accuracy (b) Gauss-Legendre level 7 of accuracy (c) Kronrod-Paterson level 6 of accuracy (d) Kronrod-Paterson level 7 of accuracy



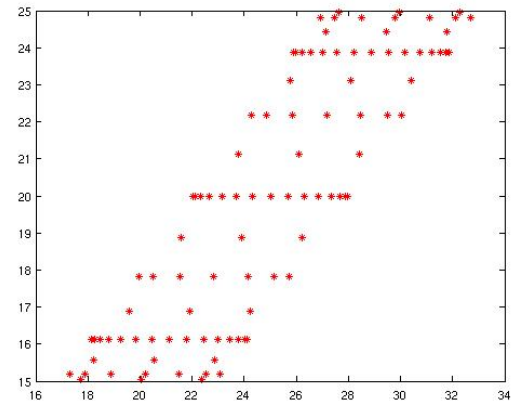
(a)



(b)

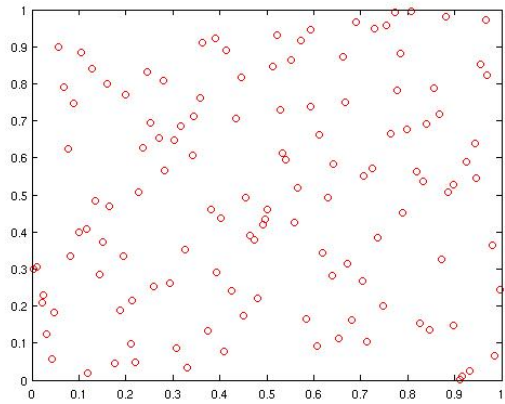


(c)

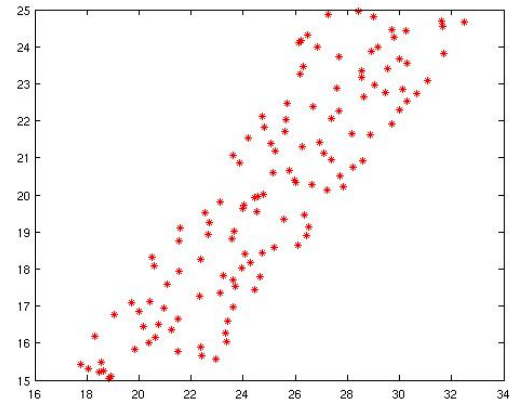


(d)

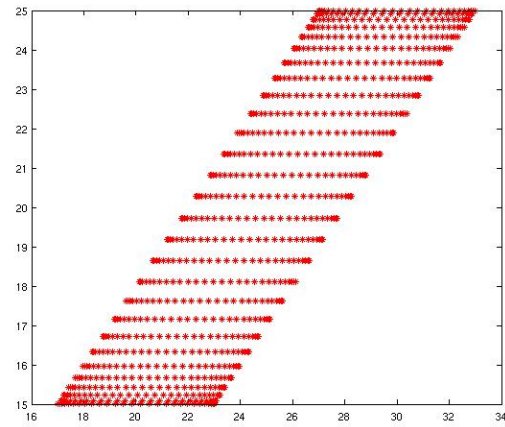
Figure 2: (a) GQU 201 grid points level 8 of accuracy (bed friction vs internal friction angle) b) KPU 97 grid points level 8 of accuracy (bed friction vs internal friction angle)



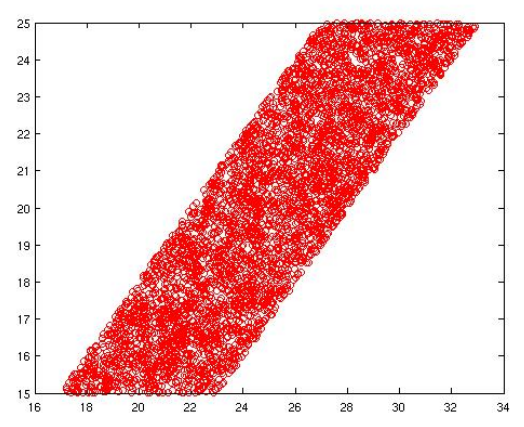
(a)



(b)



(c)



(d)

Figure 3: a) LHS 128 grid points (bed friction vs internal friction angle) b) PCQ 783 grid points c) MC 4444 grid points

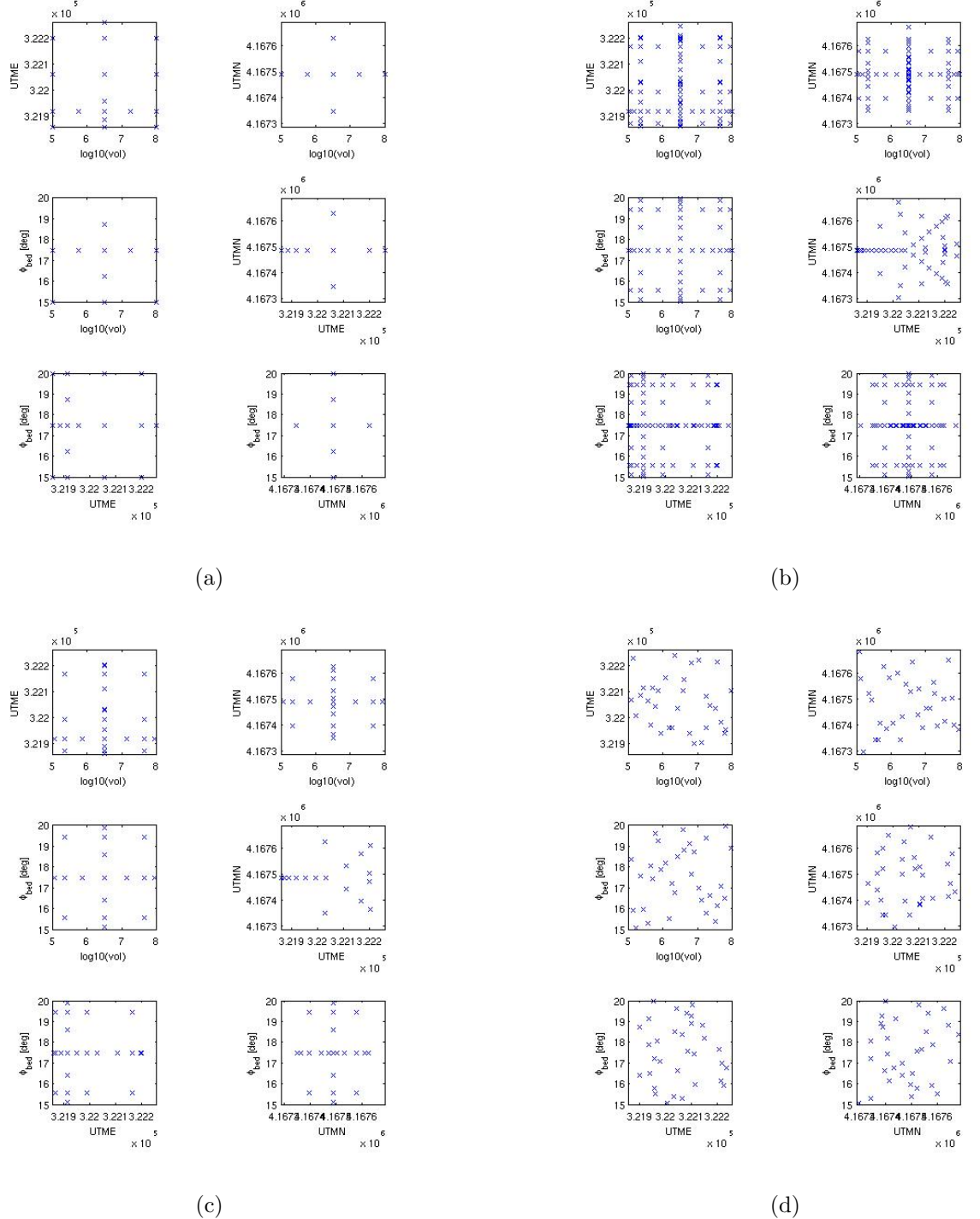


Figure 4: These plots are projections of a 4-dimensional random variable for a) CC - 32 sample points
b) CC - 114 sample points c) GP - 144 sample points (d) LHS -128 sample points

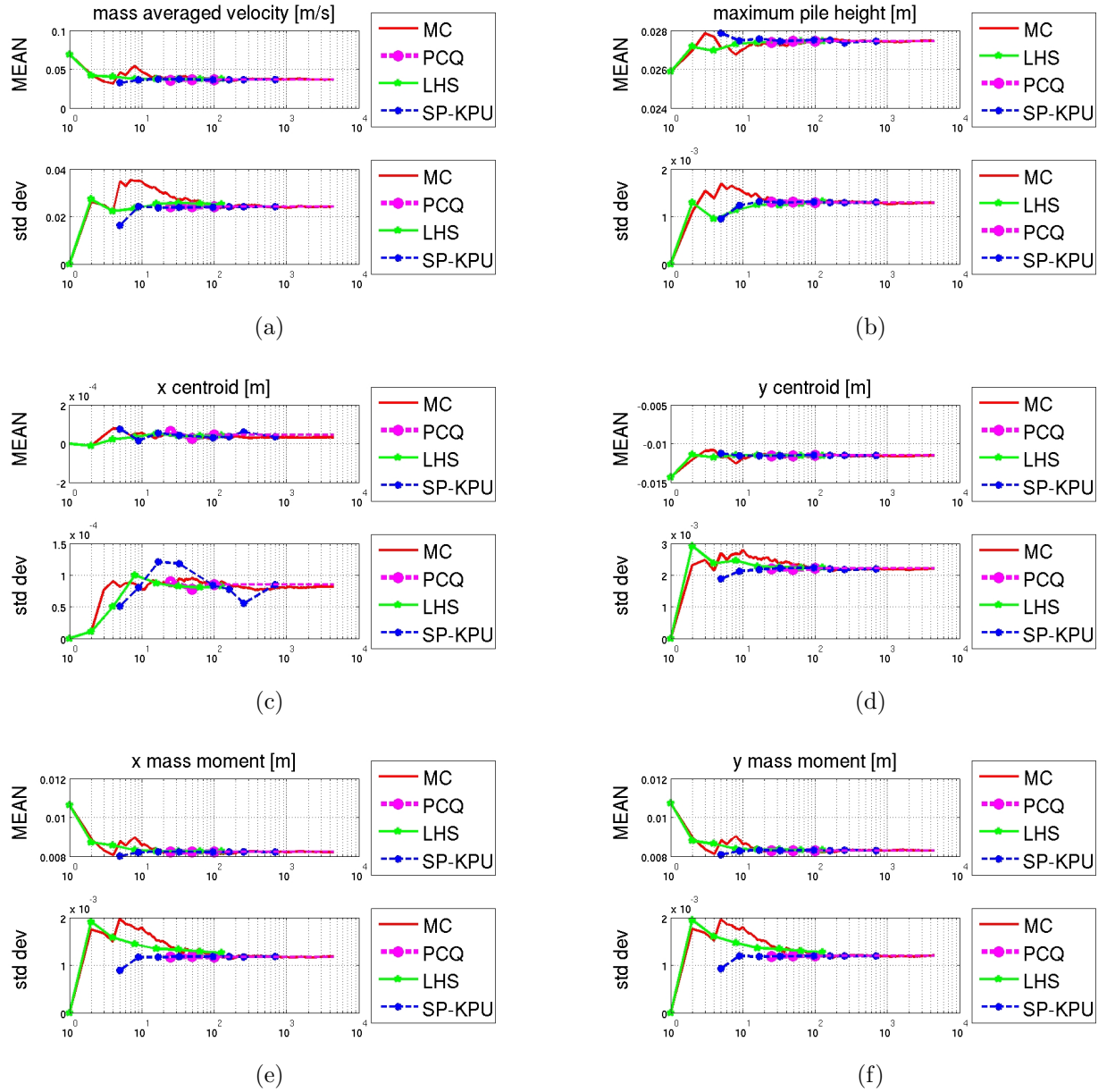


Figure 5: Convergence plot comparison for 2 RV

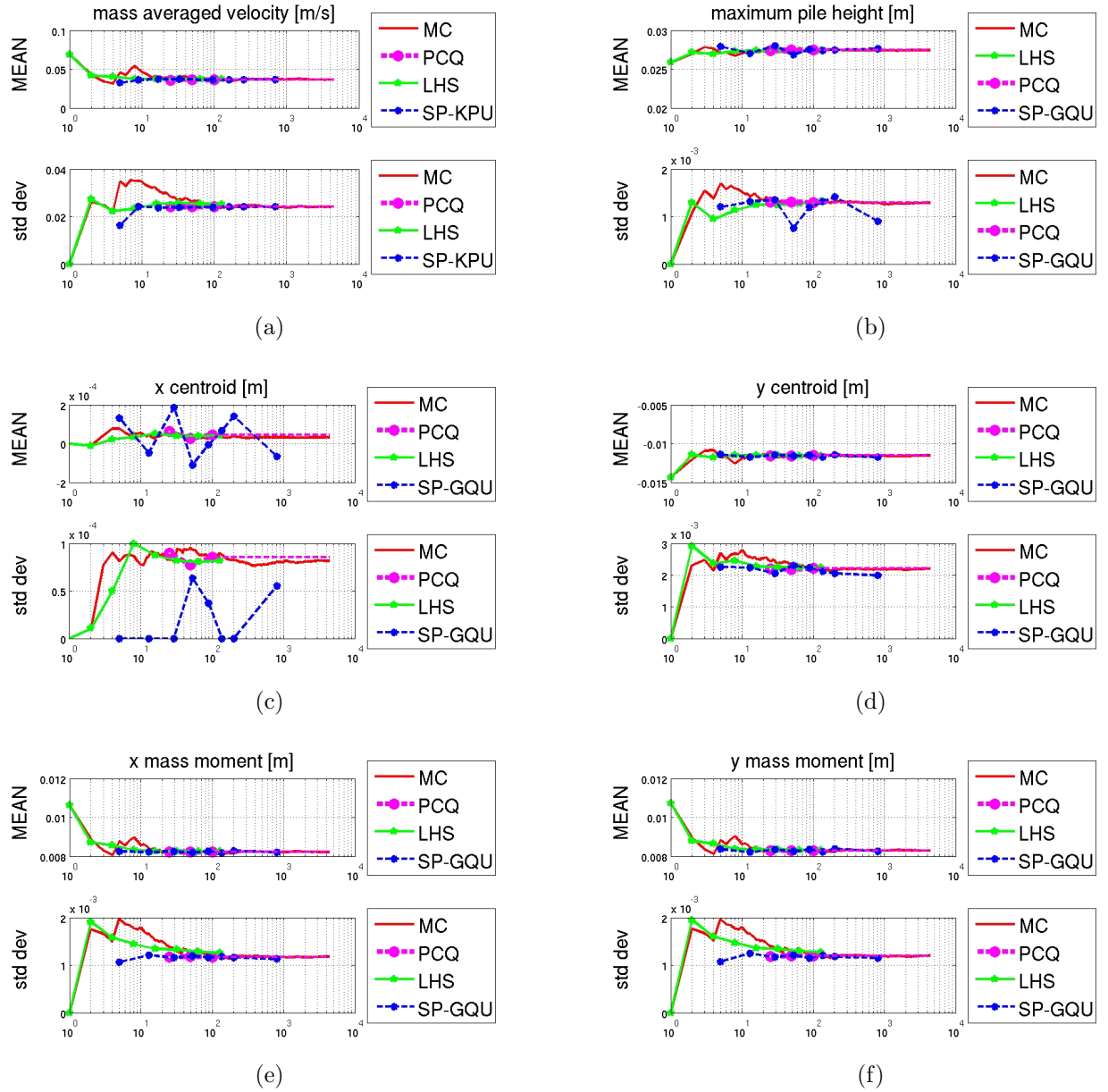


Figure 6: Convergence plot comparison for 2 RV

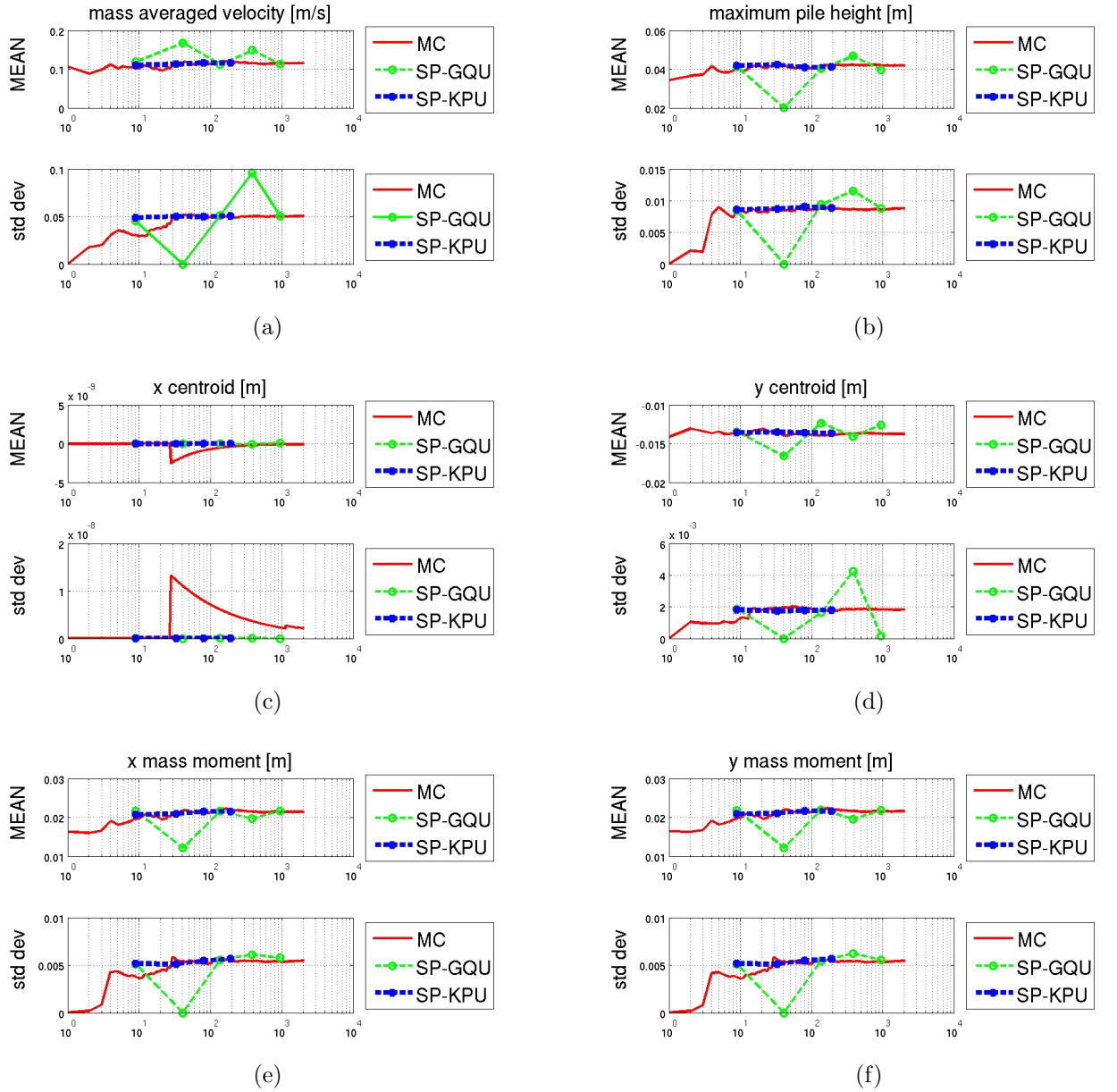


Figure 7: Convergence plot comparison for 4 RV

References

- [1] R. BAILEY, *Geologic Map of Long Valley Caldera, Mono-Inyo Craters Volcanic Chain and Vicinity, Eastern California*, Department of the Interior, Reston, VA (US), 1989.
- [2] S. BURKETT, *Geomorphic mapping and petrography of mammoth mountain, California*, Mas-

ter's thesis, State University of New York at Buffalo, 2007.

- [3] K. DALBEY, A. PATRA, E. PITMAN, M. BURSIK, AND M. SHERIDAN, *Input uncertainty propagation methods and hazard mapping of geophysical mass flow*, Journal of Geophysical Research, 113 (2008), pp. 5203–5219. doi:10.1029/2006JB004471.
- [4] B. GANAPATHYSUBRAMANIAN AND N. ZABARAS, *Sparse grid collocation schemes for stochastic natural convection problems*, Journal of Computational Physics, 225 (2007), pp. 652–685.
- [5] J. GARCKE AND M. GRIEBEL, *On the computation of the eigenproblems of hydrogen and helium in strong magnetic and electric fields with the sparse grid combination technique*, Journal of Computational Physics, 165 (2000), pp. 694–716.
- [6] M. GRIEBEL, *Adaptive sparse grid multilevel methods for elliptic pdes based on finite differences*, Computing, 61 (1998), pp. 151–179.
- [7] X. MA AND N. ZABARAS, *An adaptive hierarchical sparse grid collocation algorithm for the solution of stochastic differential equations*, Journal of Computational Physics, 228 (2009), pp. 3084–3113.
- [8] H. MATTHIES, *Stochastic finite elements: Computational approaches to stochastic partial differential equations*, Z.Angew.Math.Mech.88, 11 (2008), pp. 849–873. doi: 10.1002/zamm.200800095.
- [9] H. MURCIA, M. SHERIDAN, J. MACIAS, AND G. CORTES, *TITAN2D simulations of pyroclastic flows at Cerro Machin Volcano, Colombia: Hazard implications*, Journal of South American Earth Sciences, 29 (2010), pp. 161–170.
- [10] F. NOBILE, R. TEMPONE, AND C. G. WEBSTER, *A sparse grid stochastic collocation method for partial differential equations with random input data*, SIAM Journal on Numerical Analysis, 46 (2008), pp. 2309–2345.
- [11] A. PATRA, A. BAUER, C. NICHTA, E. PITMAN, M. F. SHERIDAN, M. BURSIK, B. RUPP, A. WEBBER, L. NAMIKAWA, AND C. RENSCHLER, *Parallel adaptive numerical simulation of dry avalanches over natural terrain*, Journal of Volcanology and Geothermal Research, 139 (2005), pp. 1–21.
- [12] S. SAVAGE AND K. HUTTER, *The motion of a finite mass of granular material down a rough incline*, Journal of Fluid Mechanics, 199 (1989), pp. 177–215.